ФИЗИКА ЭЛЕМЕНТАРНЫХ ЧАСТИЦ И АТОМНОГО ЯДРА
2011. Т. 42. ВЫП. 4

DIRECT NEUTRINO MASS MEASUREMENTS

T. Thümmler (for the KATRIN Collaboration)

Karlsruhe Institute of Technology (KIT), Institute for Nuclear Physics,
Eggenstein-Leopoldshafen, Germany

ФИЗИКА ЭЛЕМЕНТАРНЫХ ЧАСТИЦ И АТОМНОГО ЯДРА
2011. Т. 42. ВЫП. 4

DIRECT NEUTRINO MASS MEASUREMENTS

T. Thümmler (for the KATRIN Collaboration)

Karlsruhe Institute of Technology (KIT), Institute for Nuclear Physics,
Eggenstein-Leopoldshafen, Germany

The determination of the neutrino rest mass plays an important role at the intersections of cosmology, particle physics, and astroparticle physics. This topic is currently being addressed by two complementary approaches in laboratory experiments. Neutrinoless double beta decay experiments probe whether neutrinos are Majorana particles and determine an effective neutrino mass value. Single beta decay experiments such as KATRIN and MARE investigate the spectral shape of β-decay electrons close to their kinematic end-point in order to determine the neutrino rest mass with a model-independent method. Owing to neutrino flavour mixing, the neutrino mass parameter appears as an average of all neutrino mass eigenstates contributing to the electron neutrino. The KArlsruhe TRItium Neutrino experiment (KATRIN) is currently the experiment in the most advanced status of commissioning. Applying an ultra-luminous molecular windowless gaseous tritium source and an integrating high-resolution spectrometer of MAC-E-filter type, allow β-spectroscopy close to the T_2 end-point with unprecedented precision and reach a sensitivity of 200 meV/c^2 (90% CL) on the neutrino rest mass.

PACS: 23.40.-s; 14.60.Pq

INTRODUCTION

Ever since Wolfgang Pauli invented the neutrino as a desperate way out in order to understand the β-decay spectrum, its influence and importance have steadily been growing. Especially the neutrino rest mass plays an important role at the intersections of cosmology, particle physics, and astroparticle physics. In the past decades, several experiments have been performed in order to measure the masses of the three neutrino flavours (ν_e, ν_μ, ν_τ) (refer to [1] for summary tables). Until 1998, none of these experiments were able to measure the mass, thus only upper limits were given and the question of whether the neutrino has mass could not be answered.

With the following observations of flavour oscillations of atmospheric and solar neutrinos, as well as of reactor and accelerator neutrinos at long baseline, there is now a compelling evidence that neutrinos are massive. Due to this fact and owing to their large abundance in the Universe, primordial neutrinos from the Big Bang are considered as the primary candidate for hot dark matter in cosmology. Thus, they could play a specific role in the evolution of large scale structures (LSS) in the Universe. On the other hand, the on-going investigations of neutrino

properties, such as their mass hierarchy and especially their absolute mass values will open a door to the understanding of the origin of mass. Here, a precision measurement of the neutrino rest mass can discriminate between different generic ν-mass models, in particular whether they are of hierarchical type ($m_1 \ll m_2 \ll m_3$) or of quasi-degenerate type ($m_1 \simeq m_2 \simeq m_3$). Although experiments on neutrino flavour oscillation provide compelling evidence for massive neutrinos, they can only provide mixing angles and differences of squared neutrino mass eigenstates, and hence no absolute mass values.

Based on the knowledge of mixing angles and mass differences, all neutrino masses can be linked by measuring one absolute mass value only. Therefore, and owing to the smallness of the mass differences, the only appropriate way to fix m_{ν_i} is to pursue neutrino mass experiments with the highest sensitivities to sub-eV neutrino masses, i.e., experiments searching for m_{ν_e}.

In this context, cosmological investigations provide very sensitive methods to determine an estimate for the neutrino mass [2]. Since the ν-flavour itself cannot be distinguished by cosmological studies, the sum of all neutrino mass eigenstates $\sum_i m_i$ is being measured. However, while cosmological studies offer a very sensitive approach in principle, it has to be emphasized that there always remains a generic model dependence, which easily leads to factors of 2, 4 of uncertainty in the neutrino mass prediction [3, 4].

On the other hand, the purely kinematic time-of-flight analysis of neutrinos emitted in core-collapse supernovae suffers from the model dependence of the emission time as well as from low statistics. This rather attractive method can thus not compete with experiments in the sub-eV range.

At the end of the day, it is essential to perform dedicated laboratory experiments with sub-eV sensitivity and without model dependencies, in order to measure the neutrino mass.

1. DIRECT ν-MASS IN LABORATORY EXPERIMENTS

There are two well-known approaches which are complementary in their physics objectives: i) the search for neutrinoless double β-decay ($0\nu\beta\beta$), and ii) the precise spectroscopy of β-decay at its kinematic end-point.

i) The $0\nu\beta\beta$ process requires the neutrino to be its own antiparticle, which means neutrinos can be described as Majorana particles. In neutrinoless double β-decay experiments, an effective Majorana mass $m_{\beta\beta}$ is being determined, which corresponds to the coherent sum of all mass eigenstates m_i with respect to the PMNS mixing matrix U_{ei}

$$m_{\beta\beta} = \left| \sum_i U_{ei}^2 \cdot m_i \right| . \tag{1}$$

In this context the coherence implies the possibility of cancellations in $m_{\beta\beta}$, as the mass eigenvalues are weighted by the U_{ei}^2 appearing in (1) and complex CP phases. This generic fact introduces a model dependence and has to be taken into account when comparing claims or limits like $m_{\beta\beta} < 0.35$ eV/c^2 [5] to results from single β-decay experiments. For details about $0\nu\beta\beta$ experiments and the latest status, please, refer to [6, 7].

ii) Experiments investigating single β-decay offer a direct and model-independent method to determine the absolute neutrino mass. The latter rely only on the relativistic energy-momentum relation and energy conservation [8, 9]. In contrast to (1), single β-decay experiments determine the squared neutrino mass $m_{\nu_e}^2$ as incoherent sum of all mass eigenstates according to the PMNS matrix. Here, cancellations are not possible.

$$m_{\nu_e}^2 = \sum_i |U_{ei}|^2 \cdot m_i^2. \tag{2}$$

Currently, the tightest experimental upper bounds from single β-decay ($m_{\nu_e} < 2.3$ eV/c^2) have been determined in the tritium β-decay experiments in Mainz [10] and Troitzk [11]. However, both experiments have reached their sensitivity limit. At present new experiments are being assembled or designed which will increase the experimental precision by two orders of magnitude, thus increasing the sensitivity on m_{ν_e} by one order of magnitude to 200 meV/c^2.

1.1. Tritium β-Decay. The basic principle applied in the model-independent method of β-spectroscopy relies on kinematics and energy conservation only, with the squared neutrino mass eigenstate m_i^2 appearing in the phase space factor. For a detailed description including final states and relativistic kinematics we refer to [8, 9].

The following example is based on tritium beta decay:

$$T \rightarrow {}^3\mathrm{He} + e^- + \bar{\nu}_e. \tag{3}$$

Using Fermi's Golden Rule, the electron energy spectrum of tritium β-decay can be derived for each individual neutrino mass eigenstate m_i to be:

$$\frac{d\Gamma_i}{dE} = C \times F(Z+1, E)\, p\, (E + m_e c^2)(E_0 - E) \times \\ \times \sqrt{(E_0 - E)^2 - m_i^2 c^4}\, \Theta(E_0 - E - m_i c^2). \tag{4}$$

Here, E is the kinetic energy of the electron; m_e, the electron mass; and p, the electron momentum. E_0 denotes the total decay energy; $F(Z+1, E)$ is the Fermi function, which takes the Coulomb interaction of the emitted electron with the remaining nucleus into account, and $\Theta(E_0 - E - m_i c^2)$ provides energy

conservation. In addition,

$$C = \frac{G_F^2}{2\pi^3\hbar^7 c^5}\cos^2(\theta_C)|\mathcal{M}|^2 \tag{5}$$

comprises the Fermi constant G_F, the Cabibbo angle θ_C, and the nuclear matrix element $\mathcal{M}$. Equation (4) is only valid for the decay of a bare and infinitely heavy nucleus. For a more realistic description, one has to deal with atoms and molecules of finite mass. In this case, not only recoil corrections are mandatory, but one has to take into account the possibility of exciting the electron shell as well as the molecular final-state spectrum. With a probability W_j, the remaining atom or molecule will end up in an excited state of energy V_j. Hence, (4) needs to be modified into a sum of β-spectra with amplitudes W_j and modified end-point energies $E_{0,j} = E_0 - V_j$.

The nuclear matrix element $\mathcal{M}$ as well as the Fermi function $F(Z+1, E)$ are independent of m_i. The influence of m_i on the spectral shape is thus given by the phase space only. As (4) indicates, the squared mass m_i^2 is the experimental observable. However, the estimated size of the neutrino mass eigenstates m_i is small compared to the experimental resolution δE at present. Therefore, the individual mass eigenstates cannot be resolved as indicated by (4), thus only a combined spectrum can be measured according to

$$\frac{d\Gamma}{dE} = \sum_{i=1}^{3}\frac{d\Gamma_i}{dE}. \tag{6}$$

Finally, the experimental observable $m_{\nu_e}^2$ is an effective mass parameter corresponding to (2), which is derived by analyzing the spectrum close to the kinematic end-point, where $(E_0 - E)$ is small and the mass term becomes significant. A nonzero neutrino mass will not only shift the end-point, but also change the spectral shape (see Fig. 1). The count rate at the end-point is very small; and as the absolute Q-value is not known precisely enough, one has to focus on measuring the shape of the spectrum, rather than on targeting at the end-point shift. Correspondingly, only a very narrow interval close to the β-decay end-point needs to be analyzed, in order to measure a statistically significant neutrino mass value. The fraction of β-decays in this region is proportional to the third power of the end-point energy. This kind of basic properties defines the key requirements for every kind of single β-decay based neutrino mass experiment.

Concerning possible β-sources, a high primary β-decay rate is required as well as a β-emitter with the lowest possible end-point energy E_0. Of course, super-allowed or allowed transitions are preferred in order to avoid systematics from shape distortions. The detection of the β-electrons at keV end-point energies requires a very high resolution of less than a few eV in order to map the shape of the spectrum. Furthermore, the detection principle has to allow to accept a

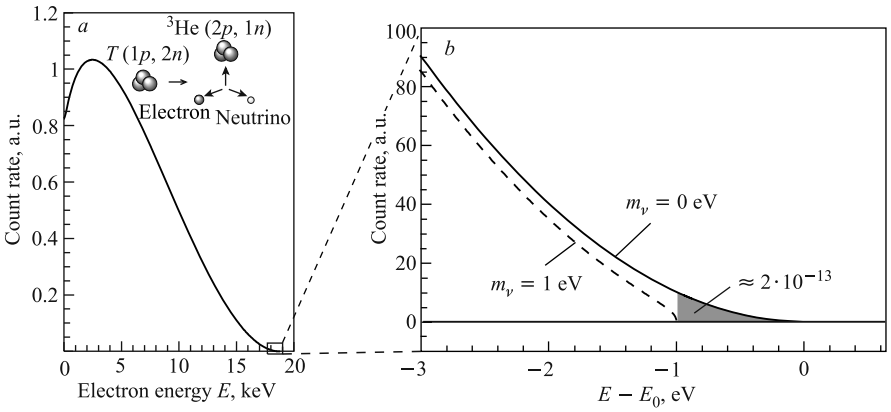

Fig. 1. Electron energy spectrum of tritium β-decay. The entire spectrum is drawn in plot *a*. In plot *b*, the region close to the end-point E_0 is magnified. Solid line is a spectrum without neutrino mass. Dashed line is a neutrino mass of 1 eV/c^2. The gray shaded triangle corresponds to a fraction of $2 \cdot 10^{-13}$ of all tritium β-decays

large part of the solid angle to maximize the available count rate in the end-point region. In any case, the lowest possible background is required in order not to cover the region of interest by noise.

There are two complementary approaches for single β-decay based neutrino mass investigations with different systematics:

1. In the calorimetric approach, the source is identical to the detector. Usually metallic or dielectric ^{187}Re crystal bolometers are used and the entire β-decay energy is being measured as a differential energy spectrum. The isotope ^{187}Re has the lowest known β-decay end-point energy at 2.47 keV. However, due to its rather long half-life of $4.3 \cdot 10^{10}$ y the specific activity is very low. In this context the advantage of bolometers is that they are modular, thus their number can be scaled up in order to increase the available amount of source material, and hence the sensitivity. The MARE experiment is following this approach as successor of the MANU and the MIBETA experiments (see Sec. 2).

2. In the spectrometer approach, source and detector are separate devices. An external tritium source is used as β-emitter, and the decay electrons are guided to the spectrometer. The kinetic energy of the β-electrons is then analyzed as integral spectrum by an electrostatic spectrometer. Here, the source material is high-purity molecular tritium T_2. Tritium has the second lowest end-point at 18.6 keV, but, in contrast to ^{187}Re, it features a short half-life of only 12.3 y, thus easily providing a high activity. The spectrometer approach, which has been used successfully in the Mainz and the Troitzk experiments, implies strict scaling

laws for the size of the spectrometer and will reach its ultimate size and precision in the KATRIN experiment.

Besides these approaches, new ideas have recently come up. The Project 8 proposal [12] aims to make use of radio-frequency spectroscopy in order to measure the kinetic energy of β-electrons from a gaseous T_2 source. Here, an array of antennas would capture the coherent cyclotron radiation emitted by the β-decay electrons when moving through a homogeneous magnetic field. This technique essentially turns the energy measurement into a precise frequency measurement, without any scale restriction as in the spectrometer approach. Futhermore, the method is non-destructive, which means that the β-electron will survive the energy measurement. In [12], the authors estimate an ultimate sensitivity of 0.1 eV for this method. Currently, a first proof-of-principle experiment is in preparation in order to show that it is feasible to detect electrons and to determine their kinetic energy with this method.

2. THE MARE EXPERIMENT

As is outlined above, MARE (Microcalorimeter Arrays for a Rhenium Experiment) uses ^{187}Re as β-emitter [13]. The exceedingly long half-life of ^{187}Re of $4.3 \cdot 10^{10}$ y — about 3 times the age of the Universe — is the result of the unique first order forbidden transition from rhenium in a $(5/2^+)$ into osmium in a $(1/2^-)$ spin and parity state [14]

$$^{187}_{85}\mathrm{Re} \rightarrow {}^{187}_{86}\mathrm{Os} + e^- + \bar{\nu}_e. \tag{7}$$

Owing to the low β-decay end-point energy at $E_0 = 2.47$ keV, ^{187}Re is about 400 times more efficient in terms of data accumulation in the region of interest close to the kinematic end-point when compared to tritium. This is a simple consequence of the third power dependence of the β-spectrum close to the end-point $N \propto (E_0)^3$. However, due to the low end-point energy and the low specific activity, the only reasonable method for ^{187}Re β-spectroscopy is the calorimetric approach. By applying multipixel arrays of bolometers, the low specific activity of individual bolometers can be circumvented. The feasibility of using cryogenic rhenium microcalorimeters has already been demonstrated by the MANU and MIBETA experiments. The latter derived the lowest calorimetric upper limit of $m_\nu < 15$ eV after accumulating 10^6 β-decays [15]. MARE is the successor of the MANU and MIBETA experiments and will be performed in two phases with increased sensitivity [13].

The goal of phase I of MARE is to improve the current sensitivity on m_ν by one order of magnitude to $m_\nu \approx 2$ eV by increasing the statistics to $\approx 10^{10}$ β-decays. The anticipated sensitivity will then be comparable to the Mainz and Troitzk experiments ($m_\nu \approx 2$ eV) and can be used to independently check their

upper limit. In this first phase both, metallic rhenium and $AgReO_4$ bolometers are being examined. Using calorimeter pixel arrays, it will take three years to obtain the intended number of decays. During this time the main objective will be to complete the R&D programme for improving the sensor technology for the next phase.

MARE phase II aims to finally improve the sensitivity again by another order of magnitude with increased statistics of 10^{14} β-decays. Reaching a sensitivity of $m_\nu \approx 0.2$ eV, MARE will be able to scrutinize a KATRIN result with a completely independent method and different systematics. However, the challenge of this project will result from the operation of 50000 bolometer pixels over a measurement time of at least 5 years in order to reach the projected sensitivity.

3. THE KATRIN EXPERIMENT

The KATRIN (KArlsruhe TRItium Neutrino) experiment [16,17] is based on the β-decay of tritium (3). Tritium offers the second lowest end-point energy of 18.6 keV, which can easily be handled in a spectrometer-based experiment, and it provides further advantages for neutrino mass investigations. The β-decay of tritium is a superallowed transition with a short half-life of 12.3 y, which is the reason for its high specific activity. Furthermore, as stated in (5) the nuclear matrix element of this transition is energy independent, thus no spectral corrections have to be taken into account. Based on the simple electronic shell configuration of tritium and its daughter ion ($^3He^+$), the final state spectrum can be calculated precisely. Especially the influence from interactions of the emitted β-electron with the source material itself can be calculated in a straightforward way. Relying on these attractive features, a long series of neutrino mass experiments has been performed in the past decades. These experiments achieved a reduction of the uncertainty of m_ν by nearly two orders of magnitude, refer to [18]. In addition, the understanding of systematic effects and improvements of the experimental setups solved the issue with negative values of m_ν^2 [9]. As mentioned above, the experiments in Mainz [10] and Troitzk [11] determined the lowest upper bound on m_ν. No further improvements are expected from these experiments as their sensitivity limit has been reached.

KATRIN represents the next generation tritium-based neutrino mass experiment. It makes use of a molecular gaseous tritium source and an electrostatic energy filter based on the MAC-E filter principle.

3.1. MAC-E Filter Principle. The MAC-E filter uses magnetic adiabatic collimation in combination with an electrostatic energy filter [19], its basic principle is shown in Fig. 2. The β-decay electrons are emitted in the source in a region of high magnetic field. The latter guides the electrons to the spectrometer, where the magnetic field drops by several orders of magnitude. Maintaining

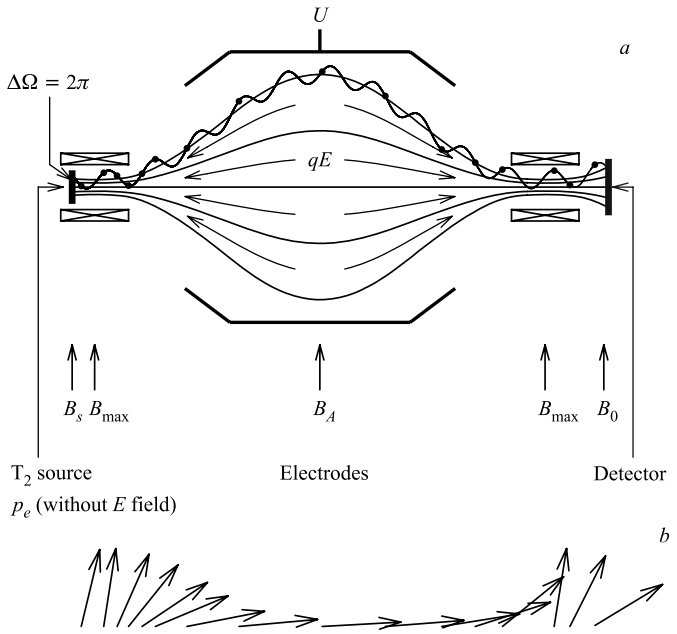

Fig. 2. MAC-E filter principle. *a*) Superconducting solenoid magnets provide the magnetic guiding field, electrodes create the electrostatic retarding potential. Electrons emitted from the source are being collimated magnetically under energy conservation, while the retarding potential slows them down and analyzes their kinetic energy as integrating high-pass filter. *b*) Magnetic adiabatic collimation represented by electron momentum vectors without retardation

a strictly adiabatic regime with full energy conservation, the magnetic gradient force transforms the cyclotron energy of the isotropically emitted electrons into the longitudinal component. This adiabatic energy transformation is realized by keeping the field gradients small along the electron's path, thus the magnetic moment μ is conserved:

$$\mu = |\boldsymbol{\mu}| = \frac{e}{2m_e}|\mathbf{l}| = \frac{E_\perp}{B} = \text{const}^*. \tag{8}$$

In the region of decreasing magnetic field B, the kinetic energy $E_\perp$ perpendicular to the magnetic field drops accordingly. Finally, almost all of the kinetic energy has been transformed into the longitudinal component $E_\parallel$, which can then be analyzed electrostatically by the retarding potential. The latter field slows down

*Equation given in nonrelativistic approximation.

the electrons by reducing their longitudinal energy and only electrons which have sufficient kinetic energy to pass this potential barrier are counted, thus the MAC-E filter acts as high-energy-pass filter for electrons.

Both effects have to be aligned very carefully for a proper energy analysis. The relative resolution of the filter is then defined by the magnetic field ratio between minimum field in the center of the spectrometer and maximum field at the pinch magnet:

$$\frac{\Delta E}{E} = \frac{B_{\min}}{B_{\max}}. \tag{9}$$

The finite width $\Delta E/E$ is essentially the remaining fraction of the perpendicular energy component, which being not completely transformed into the longitudinal part, thus defining the resolution of the MAC-E filter. Using this principle, the β-spectrum can be measured in integral form by variation of the retarding potential, or more precisely by variation of the potential difference between source and spectrometer. This defines the overall electromagnetic design of KATRIN and the size of its components.

An overview of the main beam-line is given in Fig. 3. KATRIN faces challenges in all key technologies which are applied in the experiment. As an example, about 10^{11} electrons/s are emitted in the source, while at the far detector side a

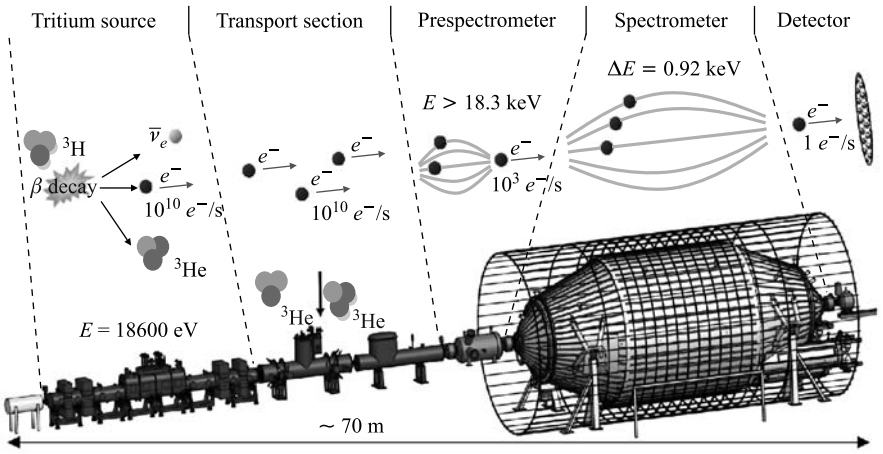

Fig. 3. Overview of the KATRIN main beam-line. High purity T_2 gas is being injected into the source tube. The transport section guides the β-decay electrons magnetically and removes remaining gas by active and cryogenic pumping. Electrons close to the end-point region can pass the prespectrometer and enter the main spectrometer for precise energy analysis. The low background Si-PIN detector system counts the transmitted electrons

background rate of the order of only 10^{-2} c.p.s. has to be reached. The source column density, temperature and pressure have to be kept stable at the 10^{-3} level. The transport section has to reduce the tritium gas flow by a huge amount of 10^{14}, in order not to increase the background in the spectrometer section. In addition, the decay electrons have to be transported fully adiabatically on the meV-scale over a distance of about 50 m. In the spectrometer region, carefully designed electromagnetic field conditions have to be implemented and maintained with the high voltage stability on the 10^{-6} scale for operating voltages up to 35 kV being one striking example. In particular, electromagnetic conditions leading to Penning-like trapping conditions have to be avoided in order to reach low background rates. The following subsection addresses the details of some key components and their present status.

3.2. The KATRIN Setup. The KATRIN setup stretches over 70 m and can be grouped into five independent components. The windowless gaseous tritium source (WGTS) provides a high activity of 10^{11} β-decays per second. There, the tritium gas is injected into the center part of the beam-tube and flows to both ends, where it is removed by turbomolecular pumps. Electrons emitted by the T_2 decay are guided by strong magnetic fields ($B = 3.6$ T in the central region and $B = 5.6$ T in the transport section) to the transport section and finally to the spectrometer section. This system is designed to retain the gas flow by 14 orders of magnitude. The prespectrometer — which provides the option to operate as MAC-E filter with moderate resolution of about 100 eV — can be used to further reduce the tritium number density considerably. In an operation mode at nonzero retarding potential, only high-energy electrons close to the end-point region would be allowed to enter the main spectrometer for the precise energy analysis. The main spectrometer is an unprecedented MAC-E filter offering a resolution of $\Delta E = 0.93$ eV for 18.6 keV electrons by applying a magnetic field ratio of $1/20000$. The latter defines the size of the main spectrometer, since the entire magnetic flux tube ratio of the source has to be analyzed.

3.2.1. Windowless Gaseous Tritium Source. In order to meet its sensitivity goal, KATRIN requires a stable source with high luminosity, and low systematic effects. The design luminosity of $1.7 \cdot 10^{11}$ Bq is equivalent to a rate of $5 \cdot 10^{19}$ T_2 molecules to be injected per second into the source tube, which adds up to a throughput of 40 g per day. These stringent design criteria are met by a unique research facility in Europe: Tritium Laboratory Karlsruhe (TLK), located at the KIT Campus North site, which also provides tritium technology for the ITER fusion facility [20]. The tritium purity for KATRIN has to be kept above 95%, the source temperature at $T = 27$ K, and the injection pressure at 10^{-3} mbar. In order to achieve a stable column density all these parameters have to be stable on the 10^{-3} level. At TLK a sophisticated tritium loop system has been commissioned for KATRIN, providing a stable injection rate and a high purity isotope separation stage. Being designed for a stability of 10^{-3}, test runs showed

that the loop system (without the final WGTS beam-tube part) reaches a 10^{-4} stability level over a 4 months time interval.

A new concept of temperature stabilization will be applied to the WGTS beam-tube ($l = 10$ m, $d = 9$ cm) in order to achieve a stability of $\Delta T \leqslant 30$ mK at the source operating temperature. The inner beam-tube is directly coupled to a two phase Ne thermosiphon [21]. This novel concept is presently being tested at the WGTS demonstrator, which is the inner part of the WGTS cryostat without superconducting magnets. After the demonstrator tests it will be integrated into the WGTS cryostat. At present, we expect the cryostat to be ready for implementation into the KATRIN beam-line in late 2012.

3.2.2. The Transport Section. Adjacent to the WGTS, the transport section guides the decay electrons to the spectrometer section by strong magnetic fields of $B = 5.6$ T. The stringent tritium retention by the factor 10^{14} is achieved in two steps. First the differential pumping section DPS uses active pumping to provide a T_2 retention of 10^7. The DPS2-F cryostat is on-site and its commissioning has recently been completed. The cryogenic pumping section CPS will make use of cryosorption to achieve a further retention of $> 10^7$. Here, the liquid He cold inner beam-tube is covered with Ar frost, providing a large surface to cryosorp the T_2. The CPS concept has been successfully tested in [22, 23] and the CPS cryostat itself is presently under construction.

3.2.3. The Prespectrometer Test Setup. The spectrometer section consists of two MAC-E filters. The prespectrometer is a MAC-E filter with sufficient resolution to allow to cut off the low energy part of the β-spectrum at about 300 eV below the end-point, if required. At present it acts as an important test setup, where all major technologies for the main spectrometer have been tested, i.e., the vacuum concept, the electromagnetic design as well as electron transmission properties and the detector concept. Especially the electromagnetic design will have a strong impact on the overall background reduction. Even tiny cm^3-sized Penning-like traps close to the ground electrode can cause substantial background rates of $> 10^3$ c.p.s. Based on the advanced KATRIN field calculation code (KASSIOPEIA), the electrode shapes have been refined to avoid these traps. This iterative process has resulted in a background level of a few 10^{-3} c.p.s., which cannot be distinguished from the intrinsic detector background, hence the prespectrometer is considered as a quasi-background free device. Remaining background features have originated from Rn decays in the volume, which result to a lesser part from auxiliary components and predominantly stem from the SEAS nonevaporable getter material required for maintaining UHV conditions. The auxiliary parts involved have been removed and Rn from the getter material has been eliminated by LN_2 baffles, for details see [24]. Finally, the prespectrometer will be integrated into the beam-line.

3.2.4. The Main Spectrometer. The main spectrometer analyzes the β-decay electrons at the end-point region with a full width of 0.93 eV. As it has to operate

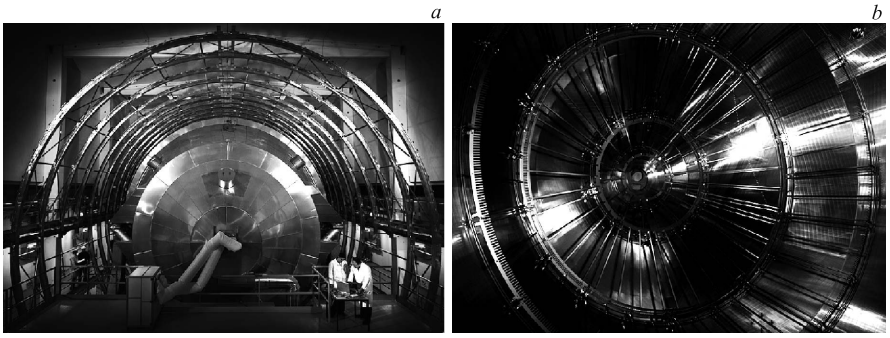

Fig. 4. *a*) View of the main spectrometer vacuum vessel and the surrounding air-coil structure. *b*) Wire electrode installation inside the main spectrometer, individual wires are barely visible on this scale

with a background rate at the 10^{-3} c.p.s. level, background from low-energy electrons created by cosmic muons in the vessel wall has to be rejected. For this purpose the dominant magnetic shielding has to be supplemented by a UHV compatible wire electrode system (240 modules, 23000 wires, 0.2 mm precision). It is currently being installed, see Fig. 4. Vacuum tank and wire electrode provide the precise retarding potential for the energy filter and are supplied by high-voltage equipment at a precision level of 10^{-6}. This level is of key importance for the ν-mass measurement, thus it will be monitored by ultra-precise high-voltage dividers [25, 26] and a separate monitor spectrometer beam-line. The latter uses the same retarding potential and measures a nuclear standard which is emitting monoenergetic electrons. Since the electromagnetic properties of the MAC-E filter are extremely sensitive to small distortions of the magnetic field, an air coil system has been installed around the spectrometer vessel. As is shown in Fig. 4, it consists of large coils and allows one to compensate the earth magnetic field and to fine tune the magnetic flux tube.

3.2.5. The Detector Setup. The transmitted electrons are counted by a detector based on a monolithic 148 pixel Si-PIN diode with an energy resolution of about 1 keV, and the ability to detect rates from 10^{-3} c.p.s. in the end-point region and up to 10^3 c.p.s. during calibration runs, while keeping the background low. The active area with 9 cm diameter is subdivided in a dartboard pattern of 12 concentric rings with 30° azimuthal segmentation.

4. KATRIN OUTLOOK AND SENSITIVITY

After commissioning and testing, the complete system integration is planned for late 2012 [27]. As soon as the setup is in measurement condition, KATRIN will take 3 years of data, which corresponds to 5 years real-time. The statistical

uncertainty is estimated to be $\Delta m^2_{\rm stat} = 0.018$ eV$^2/c^4$. Likewise, the systematic uncertainty is being restricted to $\Delta m^2_{\rm syst} < 0.017$ eV$^2/c^4$ in order to minimize the total uncertainty to $\Delta m^2_{\rm tot} = 0.025$ eV$^2/c^4$. This leads to the KATRIN design sensitivity of $m_\nu = 200$ meV$/c^2$ (90% CL) and the discovery potential of $m_\nu = 0.35$ eV$/c^2$ with 5σ significance.

5. SUMMARY

The on-going efforts to measure the absolute mass of neutrinos is well motivated by recent results in particle and astroparticle physics. Recent advances in ultrahigh β-spectroscopy offer a model-independent method for determining the ν-mass. The Re-based MARE experiment is going to check the present limits, while at the same time improving the detector technology. In future, MARE will be able to scrutinize the KATRIN result, after operating 50000 bolometer pixels for at least 5 years. New concepts for β-spectroscopy such as Project 8 will open new and independent pathways to sub-eV sensitivities and should be matured in an R&D phase. The estimated sensitivity of the tritium-based KATRIN experiment is $m_\nu = 200$ meV/c^2 (90% CL). Its construction is proceeding well with several of the major components being already on-site [27]. The complete system integration is planned for 2012.

REFERENCES

1. *Nakamura K. et al. (Particle Data Group)* // J. Phys. G. 2010. V. 37. P. 075021.
2. *Pastor S.* Light Neutrinos in Cosmology // Part. Nucl. 2011. V. 42, No. 4.
3. *Hannestad S. et al.* arXiv:1004.0695.
4. *Gonzalez-Garcia M.C. et al.* // JHEP. 2010. V. 08. P. 117; arXiv:1006.3795.
5. *Klapdor-Kleingrothaus H. V. et al.* // Eur. Phys. J. A. 2001. V. 12. P. 147.
6. *Simkovic F.* Neutrinoless Double Beta Decay and Related Topics // Part. Nucl. 2011. V. 42, No. 4.
7. *Barabash A. S.* Double Beta Decay Experiments // Part. Nucl. 2011. V. 42, No. 4.
8. *Masood S. S. et al.* // Phys. Rev. C. 2007. V. 76. P. 045501.
9. *Otten E. W., Weinheimer Ch.* // Rep. Prog. Phys. 2008. V. 71. P. 086201.
10. *Kraus C. et al.* // Eur. Phys. J. C. 2005. V. 40. P. 447.
11. *Lobashev V. M.* // Nucl. Phys. A. 2003. V. 719. P. 153c.
12. *Monreal B. et al.* // Phys. Rev. D. 2009. V. 80. P. 051301(R).
13. *Sangiorgio S. et al.* // Prog. Part. Nucl. Phys. 2006. V. 57. P. 68–70.
14. *Cosulich E. et al.* // Phys. Lett. B. 1992. V. 295. P. 143–147.
15. *Sisti M. et al.* // Nucl. Instr. Meth. A. 2004. V. 520. P. 124.
16. *Osipowicz A. et al. (KATRIN Collab.).* hep-ex/0109033.

17. *Angrik J. et al.* FZK Scientific Report. 7090;
http://bibliothek.fzk.de/zb/berichte/FZKA7090.pdf
18. *Weinheimer Ch.* arXiv:0912.1619.
19. *Picard A. et al.* // Nucl. Instr. Meth. A. 1992. V. 63. P. 345.
20. *Bornschein B. et al.* // Fusion Science and Technology. 2005. V. 48. P. 15.
21. *Grohmann S.* // Cryogenics. 2009. V. 49, No. 8. P. 413–420.
22. *Kazachenko O. et al.* // Nucl. Instr. Meth. A. 2008. V. 587. P. 136.
23. *Eichelhardt F. et al.* // Fusion Science and Technology. 2008. V. 54. P. 615.
24. *Fränkle F. M.*Thesis. 2010; http://digbib.ubka.uni-karlsruhe.de/volltexte/1000019392
25. *Thümmler T. et al.* // New J. Phys. 2009. V. 11. P. 103007.
26. *Marx R.* // IEEE Trans. Instr. Meas. 2001. V. 50, No. 2. P. 426–429.
27. *Thümmler T. et al.* arXiv:1012.2282.